

# A non-standard finite difference method for convection-diffusion singularly perturbed integro-differential equations

### P. Antony Prince, L. Govindarao, and Sekar Elango\*

Department of Mathematics, Amrita School of Physical Science, Coimbatore, Amrita Vishwa Vidyapeetham, India.

## Abstract

This paper tackles singularly perturbed second-order ordinary differential equations and parabolic part'ial differential equations with the Fredholm integral term. A non-standard finite difference method is applied the derivative terms, the trapezoidal rule treats the integral term and the backward Euler method deals with the temporal derivative phrase. The approximate numerical technique for the second-order Fredholm integro-ordinary differential (convection-diffusion type) equations provides a convergence rate of order one. The time-dependent parabolic Fredholm integro-partial differential (convection-diffusion type) equations possess a convergence rate of order one. Specific numerical examples are provided to illustrate the effectiveness of the theoretical findings.

Keywords. Singular perturbation, Convection diffusion, Fitted operator, Fredholm integral, Boundary layer.

 $\textbf{2010 Mathematics Subject Classification.} \ 65\text{G}50,\ 65\text{L}12,\ 65\text{L}70,\ 65\text{R}20.$ 

## **Notations:**

y	Solution of Equation (1.4)
Y	Fully discrete solution of (1.4)
$u_i^j = u(x_i, t_j)$	Solution of Equation (1.5)
$U_i^j$	Fully discrete solution of (1.5)
$(\Delta h)$	Mesh size in space direction
au	Mesh size in time direction
C	Positive constant independent of $(\Delta h)$ and $\epsilon$
$C^n([0,1])$	Continuously differentiable $n$ times on $[0,1]$
$C^{n,m}([0,1]\times[0,T])$	n, m- times continuously differentiable
$\ \xi\ _{\infty}$	$\max_{[0,1]}  \xi(x) ,$
$\Re$	$\max_{x \in [0,1]} \int_{0}^{1}  K(x,s)  ds$
$\begin{array}{c} y_D(x_i) \\ Y_i^D \end{array}$	Continuous solutions for a differential part in $(1.4)$
$Y_i^D$	Numerical solutions for a differential part in $(1.4)$
$y_I(x_i) \\ Y_i^I$	Continuous solutions for a integral part in $(1.4)$
$Y_i^I$	Numerical solutions a integral part in (1.4)
$u_{D_t}(x_i, t_j)$	Continuous solution of time derivative in $(1.5)$
$u_{D_x}(x_i, t_j)$	Continuous solution of spatial derivative in $(1.5)$
$u_I(x_i, t_j)$	Continuous solution of integral part in $(1.5)$
$(U_{D_t})_i^j$	Numerical solution of time derivative part in (1.5)
$(U_{D_x})_i^j$	Numerical solution of spatial derivative part in (1.5)
$(U_I)_i^j$	Numerical solution of integral part in (1.5)
-	

Received: 03 January 2025 ; Accepted: 06 October 2025.

1

<sup>\*</sup> Corresponding author. Email: e\_sekar@cb.amrita.edu.

#### 1. Introduction

In general, a differential equation created by multiplying a tiny parameter with the higher derivative term of a differential equation is referred to as a singularly perturbed differential equations (SPDEs). Such a parameter is known as the singular perturbation parameter. The solutions to these equations establish a very thin layer, referred to as either an interior or boundary layer, depending on the domain. SPDEs are extremely popular due to their widespread use in various scientific and technical fields. The major objective is to find numerical solutions for these problems to achieve accuracy and convergence. Within the finite differences framework; there are several types of numerical techniques for solving SPDEs. In [11, 20, 23, 27, 29, 36] are presented one and multidimensional singularly perturbed problems (SPPs) solved by fitted mesh and fitted operator methods. SPDEs find wide applications across various scientific and engineering fields-for instance, Udupa et al. [42] applied a singular perturbation approach to study blood flow through a stenosed artery under body acceleration, while Govindarao and Sekar [13] employed numerical methods to analyze an RLC closed series circuit with small inductance values.

Integro-differential equations (IDEs) are important in domains including physics, engineering, biology and chemistry [1, 2, 35, 38]. IDEs are divided into two types based on their components: Fredholm integro-ordinary differential equations (FIODEs), which contain integral terms with a finite range and Volterra integro-ordinary differential equations (VIODEs), which contain integral terms that are bound by respected variables. A wide variety of analytical and numerical techniques developed to provide exact and approximate solutions for FIODEs and plenty of innovative numerical techniques specifically created for solving FIODEs can be found in the literature. Chen et al. proposed a Galerkin method to solve FIODEs and analyze the behaviour of the solution in [7]. In [3] Akyuz-Dascioglu et al. solved linear FIODEs by the Taylor polynomial method.

Authors of [19], consider the stochastical financial model of the Black-Scholes equation with the value of  $W = W(S, \tau)$ , which is a European call option, where  $W(S, \tau)$  denotes the value of a contingent claim with current time  $\tau$  that is dependent on the price of the underlying asset S,

$$\frac{\partial W}{\partial \tau} + \frac{1}{2}\sigma^2 S^2 \frac{\partial^2 W}{\partial S^2} + rS \frac{\partial W}{\partial S} - rW = 0, \quad (s, \tau) \in (0, \infty) \times (0, T], \tag{1.1}$$

with the initial and boundary financial conditions,

$$W(S,T) = \max(S,T) = \max(S-E,0), \quad S \in \mathbb{R}^+,$$
  
$$W(0,\tau) = 0, \quad W(S,\tau) \to S \quad \text{for} \quad S \to \infty, \quad \tau \in [0,T).$$

Here  $\sigma$  is volatility, E is the exercise price, T is the expiry time and r is the interest rate. Applying the transformations

$$S = E \exp(x), \quad \tau = T - tr^{-1}, \quad W = Ez(x, t),$$

and introducing the notation  $k = 2\sigma^{-2}r$ ,  $t^* = rT$ , the Equation (1.1) is transformed into the following dimensionless parabolic equation in the new variables  $x, \tau$ :

$$Lz(x,\tau) \equiv \left\{ \frac{\partial^2}{\partial x^2} + (k-1)\frac{\partial}{\partial x} - k - k\frac{\partial}{\partial \tau} \right\} z(x,\tau) = 0, \quad (x,\tau) \in \mathbb{R} \times (0,\tau^*],$$

with the initial condition

$$z(x,0) = \varphi_z(x), \quad x \in \mathbb{R},$$

where

$$\varphi_z(x) = \max(\exp(x) - 1, 0), \quad x \in \mathbb{R},$$

and with the condition at infinity

$$\begin{cases} z(x,\tau) \to 0, & \text{for } x \to -\infty, \\ z(x,\tau) \to \exp(x), & \text{for } x \to \infty, \quad \tau \in (0,\tau^*]. \end{cases}$$



Now, set  $\tau = t/r$ , so  $\frac{\partial}{\partial \tau} = r \frac{\partial}{\partial t}$ . Substituting these into the above equation, we obtain:

$$\left\{ \frac{\partial^2}{\partial x^2} + (k-1)\frac{\partial}{\partial x} - k - kr\frac{\partial}{\partial t} \right\} z(x,t) = 0.$$

Now divide through by kr to normalize:

$$\left\{\frac{1}{kr}\frac{\partial^2}{\partial x^2} + \frac{k-1}{kr}\frac{\partial}{\partial x} - \frac{1}{r} - \frac{\partial}{\partial t}\right\}z(x,t) = 0.$$

Introduce the small parameter  $\epsilon = \frac{1}{2}\sigma^2 r^{-1} \in (0,1)$ . Since  $k = 2\sigma^{-2}r$ , it follows that:

$$\frac{1}{kr} = \epsilon, \quad \frac{k-1}{kr} = (1-\epsilon).$$

Then the equation becomes:

$$Lz(x,t) = \left\{ \epsilon \frac{\partial^2}{\partial x^2} + (1 - \epsilon) \frac{\partial}{\partial x} - 1 - \frac{\partial}{\partial t} \right\} z(x,t) = 0, \quad (x,t) \in \mathbb{R} \times (0,t^*]$$

with initial and boundary conditions:

$$\begin{cases} z(x,0) = \max(\exp(x) - 1, 0), & x \in \mathbb{R}, \\ z(x,t) \to 0, & \text{for } x \to -\infty, \\ z(x,t) \to \exp(x), & \text{for } x \to \infty, & t \in (0, t^*], \end{cases}$$

Here,  $\epsilon = 2^{-1}\sigma^2 r^{-1}$  is a dimensionless "perturbation" parameter,  $\epsilon \in (0,1)$ .

Next, the application of the singularly perturbed Fredholm integro-partial differential equations (SPFIPDE) is formulated as follows:

$$\frac{\partial W}{\partial \tau} + \frac{1}{2}\sigma^2 S^2 \frac{\partial^2 W}{\partial S^2} + (r - \lambda \kappa) S \frac{\partial W}{\partial S} - (r + \lambda) W + \lambda \int_0^\infty W(S\eta) g(\eta) \, d\eta = 0, \quad (s, \tau) \in (0, \infty) \times (0, T]. \tag{1.2}$$

Equation (1.2) is a stochastic partial integro-differential equation model for option pricing in jump-diffusion and exponential Levy model, it is mentioned in [15]. Here  $W(S,\tau)$  denotes the value of a contingent claim with current time  $\tau$  that is dependent on the price of the underlying asset S, r is the risk-free interest rate,  $\lambda$  is the intensity of the independent Poisson process,  $g(\eta)$  is the probability density function of the jump with amplitude  $\eta$  with properties that for all  $\eta, g(\eta) \geq 0$ ,  $\int\limits_0^\infty g(\eta) \, d\eta = 1$  and  $\kappa = e^{\mu_J + \frac{\sigma_J^2}{2}} - 1$ , where  $\mu_J$  is a mean and  $\sigma_J^2$  is the variance of jump in return.

Using change the variable  $x = \ln\left(\frac{S}{K}\right)$  and  $y = \ln(\eta)$ , where K is strike price and  $t = T - \tau$ . Define the transformed function  $z(x,t) = W(Ke^x, T-t)$  and  $f(y) = g(e^y)e^y$ . Under this transformation, the integral term  $\int_0^\infty W(S\eta)g(\eta)\,d\eta$ 

becomes  $\int_{-\infty}^{\infty} z(x+y,t)f(y) dy$ , which is a convolution in log-space. This also transforms the differential operators accordingly, and Equation (1.2) becomes:

$$\frac{\partial z}{\partial t} = \frac{1}{2}\sigma^2 \frac{\partial^2 z}{\partial x^2} + \left(r - \frac{\sigma^2}{2} - \lambda\kappa\right) \frac{\partial z}{\partial x} - \left(r + \lambda\right)u + \lambda \int_{-\infty}^{\infty} z(y, t)f(y - x) \, dy. \tag{1.3}$$

The price of a European put option's initial condition and asymptotic behaviour are explained by

$$z(x,0) = \max(K - Ke^x, 0),$$

$$z(x,t) = \begin{cases} Ke^{-rt} - Ke^x, & x \to -\infty, \\ 0, & x \to \infty. \end{cases}$$



Further, if we take  $\epsilon = \frac{\sigma^2}{2}$  as a dimensional parameter in Equation (1.3), it becomes

$$\frac{\partial z}{\partial t} = \epsilon \frac{\partial^2 z}{\partial x^2} + (r - \epsilon - \lambda \kappa) \frac{\partial z}{\partial x} - (r + \lambda)u + \lambda \int_{-\infty}^{\infty} z(y, t) f(y - x) \, dy.$$

The transformation equation inspired us to form our singularly perturbed Ferdholm partial integro-differential equations. Based on these motivations our objectives are to present, second-order convection diffusion singularly perturbed integro-ordinary differential equations (SPFIODEs) in Equation (1.4) and time-dependent parabolic convection-diffusion type SPFIPDEs in Equation (1.5).

Consider, a class of linear second-order convection-diffusion SPFIODEs of the form,

$$\begin{cases}
-\epsilon y''(x) + a(x)y'(x) + b(x)y(x) + \lambda \int_{0}^{1} K(x,s)y(s) \, ds = f(x), & 0 < x < 1, \\
y(0) = A, & y(1) = B,
\end{cases}$$
(1.4)

where  $0 < \epsilon \ll 1$ ,  $\lambda$  is a given parameter. The function  $a(x) \ge \alpha > 0$ ,  $b(x) \ge 0$ , f(x) are smooth functions, K(x,s) is a kernel function and A, B are constants.

Next, define a class of convection-diffusion SPFIPDEs of parabolic type is considered as follows,

$$\begin{cases}
\left(\frac{\partial}{\partial t} + L_{\epsilon,x} + I_x\right) u(x,t) = f(x,t), & (x,t) \in Z \equiv \Omega \times (0,T] \equiv (0,1) \times (0,T], \\
u(x,0) = u_0(x), & x \in \overline{\Omega}, \\
u(0,t) = u(1,t) = 0, & t \in [0,T],
\end{cases} \tag{1.5}$$

where

$$L_{\epsilon,x}u(x,t) = -\epsilon u_{xx}(x,t) + a(x,t)u_x(x,t) + b(x,t)u(x,t), \quad 0 < \epsilon \ll 1,$$

$$I_x u(x,t) = \lambda \int_0^1 K(x,s) u(s,t)ds,$$

where  $a(x,t) \ge \alpha > 0$ ,  $b(x,t) \ge 0$ , f(x,t) are in  $C^{4,2}(\overline{Z})$ , a(x,t) is independent of t, K(x,s) is kernal function and  $\overline{Z}$  is closure of Z. Applying the compatibility conditions, the solution u(x,t) of Equation (1.5) exhibits a layer at the boundary values.

In solving SPDEs, standard techniques based on equal step lengths produce erroneous results. They are unstable and unsatisfactory in the majority of circumstances [22, 32–34, 40]. Therefore many researchers solve SPDEs numerically in [6, 24, 30, 31, 37]. Similarly, SPFIODEs show the same features. Therefore, certain researchers utilise numerical techniques to solve SPFIODEs.

Lange and Smith [18] derived the existence and uniqueness of SPFIODEs. Interpolating quadrature rules worked by Cimen et al. [8] to compute SPFIODEs with uniform mesh. A numerical solution for the non-linear first-order singularly perturbed VIODEs developed by Sevgin [39]. Amiraliyev et al. [5] developed a method to calculate error estimates that are consistent across different parameters for estimating solutions of first-order SPFIODEs with uniform mesh and also developed a customized differentiation technique in second-order SPFIODEs with Shishkin mesh [4]. The second-order reaction-diffusion SPFIODEs investigated by Durmaz et al. [10] using a fitted homogeneous type difference scheme on a Shishkin mesh reached a second-order non-optimal rate of convergence. Sekar Elango et al. [38] successfully solved the second-order reaction-diffusion SPFIODEs, using a central difference scheme applied for the second-order derivative part and integral component used by the composite trapezoidal rule of non-uniform meshes like Shishkin mesh, Bakhvavov-Shishkin mesh. They achieve a rate of convergence of order two. Later, they used a post-processing technique to change the rate of convergence from two to four. Govindarao et al. [12] handled the reaction-diffusion SPFIODEs with integral boundary conditions. The second-order derivative is constructed using a central difference scheme, while the integral component is determined using the composite trapezoidal rule of non-uniform Shishkin-type meshes. They succeeded in attaining a second-order convergence rate and later by applying the



extrapolation technique a fourth-order convergence rate is obtained. Prince et al. [28] solved the system of SPFIDE with a uniform mesh.

Due to the presence of a tiny parameter  $\epsilon$  multiplying the highest-order derivative, standard finite difference methods often fail to provide accurate solutions when  $\epsilon$  is very small. The purpose is to solve SPFPIDEs with high accuracy, therefore our approach is to change from finite difference to non-standard finite difference for tiny parameter  $\epsilon$ .

This article aims to get a convergence rate of order one for the second-order convection diffusion SPFIODEs and parabolic convection-diffusion SPFIPDEs. Initially, a non-standard finite difference (NSFD) scheme is used for the derivative part and the trapezoidal rule applies to an integral part of the uniform mesh. Hence, the Equation (1.4) converges with order one when using N mesh points. Similarly Equation (1.5) is solved by NSFD scheme with N number of mesh points in spatial and M number of mesh points in the time direction, as the results the rate of convergence of order one in the time and spatial directions, it is shown theoretically. Then the global convergence rate of order one is shown computationally.

In this article section 2 presents the stability of the Second-order SPFIODEs and its numerical discretization through a non-standard finite difference for the differential part and trapezoidal rule for the integral term, followed by the parabolic SPFIPDEs in section 3, employing the backward Euler method for time discretization and the NSFD method for spatial discretization. The trapezoidal rule approaches the integral part, followed by an estimation of the error analysis and the verification of the numerical simulations.

# 2. Second order SPFIODE

In this section consider the singularly perturbed linear second-order Fredholm integro-ordinary differential equations of the form Equation (1.4). The solution y(x) of Equation (1.4) generally occurs near the boundary layer x = 1 for tiny values of  $\epsilon$ . The stability analysis of the solution is based on the following lemma.

**Lemma 2.1** (Stability). Assume that  $a(x), f(x) \in C^n([0,1]), \frac{\partial^n}{\partial x^n} K(x,s) \in C([0,1] \times [0,1]), (n=0,1,2,3,4)$  and  $|\lambda| < \frac{\alpha}{\Re}$ . Then, the solution y(x) of Equation (1.4) satisfies the inequalities

(i) 
$$||y||_{\infty} \leq C_0$$
,

where 
$$C_0 = \left(|B - A| + \left(\frac{1}{\alpha} \|f\|_{\infty}\right) + \left(\frac{1}{\alpha} |A| \|b\|_{\infty}\right) + |A|\right) \left(1 - \left(\frac{|\lambda|\Re}{\alpha}\right)\right)^{-1}$$
 and (ii)  $|y^{(n)}(x)| \le C \left[1 + \frac{1}{\epsilon^n} \exp\left(\frac{-\alpha(1-x)}{\epsilon}\right)\right], x \in [0,1].$ 

*Proof.* Set 
$$z(x) = y(x) - A$$
 for  $0 \le x \le 1$  and  $F(x) = f(x) - \lambda \int_{0}^{1} K(x, s)y(s) ds$ .

Then 
$$z(0) = 0$$
,  $z(1) = B - A$ ,

$$|Lz(x)| = |F(x) - Ab(x)| \le ||F(x)||_{\infty} + A||b||_{\infty},$$

Using comparison principle to bound |z(x)| by the barrier function (Pg.no 25, [41])

$$\theta(x) = \frac{x}{\alpha} (\alpha |B - A| + ||F(x)||_{\infty} + |A| ||b||_{\infty}),$$

This implies  $|z(x)| \le \theta(x)$ ,  $\forall x \in [0, 1]$ .

Note that:  $||F(x)||_{\infty} \le ||f||_{\infty} + |\lambda| \max_{x \in [0,1]} \int_{0}^{1} |K(x,s)| ds ||y||_{\infty}.$ 

Then it follows,

$$||y||_{\infty} \leq C_0.$$

The next bound of  $|y^{(n)}(x)|$  is followed by the induction hypothesis, this proof technique is the same as the Kellogg and Tsan technique [16].



**Lemma 2.2.** For all integer w on a fixed mesh, it gives

$$\lim_{\epsilon \to 0} \max_{1 \le i \le N-1} \left( \frac{e^{-\frac{C}{\sqrt{\epsilon}}x_i}}{\epsilon^{\frac{w}{2}}} \right) = 0 \ \ and \ \ \lim_{\epsilon \to 0} \max_{1 \le i \le N-1} \left( \frac{e^{-\frac{C}{\sqrt{\epsilon}}(1-x_i)}}{\epsilon^{\frac{w}{2}}} \right) = 0,$$

where  $x_i = i(\Delta h)$ .

*Proof.* One can find proof of this lemma in [25].

2.1. Numerical discretization for second-order SPFIODEs. On [0,1], the uniform mesh step  $\Delta h$  is used to discretize the interval. Here  $\Delta h := \frac{1}{N}$  such that  $x_i = i(\Delta h)$ , where N is a number of finite mesh points. For each mesh point the Equation (1.4) becomes

$$-\epsilon y''(x)\big|_{x=x_i} + a(x_i)y'(x)\big|_{x=x_i} + b(x_i)y(x_i) + \lambda \int_0^1 K(x_i, s)y(s) \, ds = f(x_i), \quad i = 0, 1, \dots, N.$$
 (2.1)

Let the differential part in Equation (2.1)  $-\epsilon y'' + a_i y' + b_i y = 0$ . This equation has two linearly independent solutions  $\exp(\gamma_1 x)$  and  $\exp(\gamma_2 x)$ , where the roots of the associated characteristic equation are

$$\gamma_{1,2} = \frac{-a_i \pm \sqrt{a_i^2 + 4b_i \epsilon}}{-2\epsilon}.$$

Thus, setting  $y_i = y(x_i)$ , the theory of difference equations shows that the second order linear difference equation

$$\begin{vmatrix} y_{i-1} & \exp(\gamma_1 x_{i-1}) & \exp(\gamma_2 x_{i-1}) \\ y_i & \exp(\gamma_1 x_i) & \exp(\gamma_2 x_i) \\ y_{i+1} & \exp(\gamma_1 x_{i+1}) & \exp(\gamma_2 x_{i+1}) \end{vmatrix} = 0,$$

or equivalently

$$-\exp\left(-\frac{a_i(\Delta h)}{2\epsilon}\right)y_{i+1} + 2\cosh\left(\frac{(\Delta h)\sqrt{a_i^2 + 4b_i\epsilon}}{2\epsilon}\right)y_i - \exp\left(\frac{a_i(\Delta h)}{2\epsilon}\right)y_{i-1} = 0,$$

is an exact scheme of the original differential equation [21], after suitable manipulations, the scheme

$$-\epsilon \frac{y_{i+1} - 2y_i + y_{i-1}}{\frac{\epsilon(\Delta h)}{a_i} \left( \exp\left(\frac{a_i(\Delta h)}{\epsilon}\right) - 1 \right)} + a_i \frac{y_i - y_{i-1}}{\Delta h} + b_i y_i = 0.$$

Therefore, we obtain

$$-\epsilon y''(x)\big|_{x=x_i} + a_i y'(x)\big|_{x=x_i} + b_i y_i = -\epsilon \frac{y_{i+1} - 2y_i + y_{i-1}}{\psi_i^2} + a_i \frac{y_i - y_{i-1}}{\Delta h} + b_i y_i,$$
(2.2)

where,  $\psi_i^2 = \frac{\epsilon(\Delta h)}{a_i} \left( \exp\left(\frac{a_i(\Delta h)}{\epsilon}\right) - 1 \right)$ ,  $y_i = y(x_i)$ ,  $a_i = a(x_i)$  and  $b_i = b(x_i)$ .

Let  $g(x,s) = K(x,s)y(s) \in C^2([0,1] \times [0,1])$ , the Newton-Cotes quadrature formula of order n=1 is applied in integral part of Equation (2.1), then

$$\int_{0}^{1} g(x_i, s) ds \simeq \frac{1}{2} [g(x_i, 0) + g(x_i, 1)].$$

To increase the accuracy, apply the higher-order Newton-Cote rule. Let  $s_j = j(\Delta h)$  be an equidistant subdivision with step size  $\Delta h = \frac{1}{N}$ , where  $j = 0, 1, \dots, N$ . Then

$$\int_{0}^{1} g(x_{i}, s) ds \simeq T_{(\Delta h)} g(x_{i}, s) := (\Delta h) \left[ \frac{1}{2} g(x_{i}, s_{0}) + g(x_{i}, s_{1}) + \dots + g(x_{i}, s_{N-1}) + \frac{1}{2} g(x_{i}, s_{N}) \right]. \tag{2.3}$$



This is known as the composite trapezoidal rule.

In Equation (2.1) substitute Equations (2.2) and (2.3) then,

$$-\epsilon \frac{y_{i+1} - 2y_i + y_{i-1}}{\psi_i^2} + a(x_i) \frac{y_i - y_{i-1}}{\Delta h} + b(x_i)y(x_i) + \lambda \sum_{i=0}^{N} \theta_j(\Delta h) K(x_i, s_j) y(s_j) = f(x_i),$$
(2.4)

where  $y_i = y(x_i)$ ,  $\theta_j = \begin{cases} \frac{1}{2} & \text{for } j = 0, N, \\ 1 & \text{for } j = 1, 2, \cdots, N-1. \end{cases}$ The Equation (2.4) forms a system of linear equation MY = b. Solving this linear system by the following Algorithm 1.

# Algorithm 1 Numerical Solution of second-order SPFIODE

- 1: function solve\_linear\_system(M, b)
- 2:  $[N, N] \leftarrow \mathtt{size}(A)$
- 3: **Input:**  $M = m[i, j], Y = y_i, b = f_i$
- 4: Boundary\_conditions:  $y_0 = A$ ,  $y_N = B$
- 5: Output:  $Y \leftarrow M \setminus b$
- 2.2. Error analysis for second-order SPFIODEs. Here,  $y(x_i)$  is the continuous solution and  $Y_i$  is the numerical solution for each mesh point of Equation (1.4). The solution is split into a differential part and an integral part and the error estimation follows like

$$|y(x_i) - Y_i| = |(y_D(x_i) + y_I(x_i)) - (Y_i^D + Y_i^I)|,$$

where  $y_D(x_i), y_I(x_i)$  are the continuous solutions for a differential and integral part, similarly  $Y_i^D, Y_i^I$  are the numerical solutions for the differential part and integral part. The following lemma shows the error estimate of the differential

**Lemma 2.3.** If  $y_D(x_i)$  is the continuous solution for the differential part and  $Y_i^D$  is the numerical solution for the differential part. Then the NSFD scheme is uniformly  $\epsilon$ -convergent of order one.

i.e, 
$$\sup_{0 \le \epsilon \le 1} \max_{0 \le i \le N} |y_D(x_i) - Y_i^D| \le C(\Delta h),$$

where C is an independent constant of  $\epsilon$  and  $\Delta h$ .

Proof.

$$L_{\epsilon}^{N}(y_{i} - Y_{i}) = (L_{\epsilon,x} - L_{\epsilon,x}^{N})y_{i},$$

$$= -\epsilon y_{i}'' + a_{i}y_{i}' - \left[\epsilon \frac{y_{i+1} - 2y_{i} + y_{i-1}}{\psi_{i}^{2}}\right] - a_{i}\left[\frac{y_{i} - y_{i-1}}{\Delta h}\right].$$
(2.5)

Using proper Taylor series expansions and considering the truncated Taylor expansion  $\frac{1}{\psi_i^2} = \frac{1}{(\Delta h)^2} - \frac{a_i}{2\epsilon(\Delta h)} + \frac{a_i^2}{12\epsilon^2}$ . Then the Equation (2.5) becomes,

$$L_{\epsilon}^{N}(y_{i} - Y_{i}) = -\epsilon y_{i}^{"} + \left[ \left( \frac{\epsilon}{(\Delta h)^{2}} - \frac{a_{i}}{2(\Delta h)} + \frac{a_{i}^{2}}{12\epsilon} \right) \left( (\Delta h)^{2} y_{i}^{"} + \frac{(\Delta h)^{4}}{12} y^{""}(\eta_{i}) \right) \right] + \frac{a_{i}(\Delta h)}{2} y_{i}^{"},$$

$$\left| L_{\epsilon}^{N}(y_{i} - Y_{i}) \right| \leq \left| \frac{\epsilon(\Delta h)^{2}}{12} y^{""}(\eta_{i}) \right| + \left| \frac{a_{i}(\Delta h)^{3}}{24} y^{""}(\eta_{i}) \right| + \left| \frac{a_{i}^{2}(\Delta h)^{2}}{12\epsilon} y_{i}^{"} \right| + \left| \frac{a_{i}^{2}(\Delta h)^{4}}{144\epsilon} y^{""}(\eta_{i}) \right|,$$

where  $\eta_i \in (x_{i-1}, x_{i+1})$  and using the reation  $(\Delta h) > (\Delta h)^2 > (\Delta h)^4$  and also using Lemma 2.1 and 2.2, then it follows,

$$|L_{\epsilon}^{N}(Y_{i}-y_{i})| \leq C(\Delta h).$$

The result follows from the above truncation error analysis, as in [22].



**Lemma 2.4.** Let  $g: C^2([0,1] \times [0,1]) \to \mathbb{R}$  be twice continuously differentiable. Then the error for the composite trapezoidal rule is

$$\int_{0}^{1} K(x_{i}, s)y(s) ds - T_{(\Delta h)}g(x_{i}, s) = \frac{-1}{12} (\Delta h)^{2} \left| \frac{\partial^{2}}{\partial \xi^{2}} K(x_{i}, \xi)y(\xi) \right|, \ \xi \in [0, 1].$$

*Proof.* The proof of this lemma can be found in (Pg.no 299, [17]).

**Lemma 2.5.** If  $y_I(x_i)$  is the integral part continuous solution and  $Y_i^I$  is the integral part numerical solution. Then composite trapezoidal rule is convergent of order two.

i.e, 
$$\sup_{0 \le i \le N} |y_I(x_i) - Y_i^I| \le C(\Delta h)^2$$
,

where C is an independent constant of  $\Delta h$ .

*Proof.* Using Lemma 2.4 and  $|\lambda| < \frac{\alpha}{\Re}$ , then

$$\sup_{0 \le i \le N} |y_I(x_i) - Y_i^I| = \max_{0 \le x_i \le 1} \left| \lambda \int_0^1 K(x_i, s) y(s) \, ds - \lambda T_{(\Delta h)} g(x_i, s) \right|,$$

$$\le \frac{1}{12} |\lambda| (\Delta h)^2 \max_{0 \le x_i, s \le 1} \left| \frac{\partial^2}{\partial s^2} [K(x_i, s) y(s)] \right|,$$

$$\le C(\Delta h)^2.$$

**Theorem 2.6.** Let  $y(x_i)$  and  $Y_i$  be the continuous and numerical solution of the Equations (2.1) and (2.4) respectively. Then

$$\sup_{0 < \epsilon < 1} \max_{0 \le i \le N} |y(x_i) - Y_i| \le C(\Delta h),$$

where C is an independent constant of  $\epsilon$  and  $\Delta h$ .

*Proof.* From Lemma 2.3 and 2.5 can be used to formulate the convergence following the result,

$$\sup_{0 < \epsilon < 1} \max_{0 \le i \le N} |y(x_i) - Y_i| = |(y_D(x_i) + y_I(x_i)) - (Y_i^D + Y_i^I)|,$$

$$\leq |y_D(x_i) - Y_i^D| + |y_I(x_i) - Y_i^I|,$$

$$\leq C(\Delta h).$$

2.3. Numerical result for second order SPFIODEs. According to the theoretical analysis, the developed method exhibits a uniform first-order convergence rate, independent of the perturbation parameter  $\epsilon$ . To validate its efficiency, numerical experiments were conducted using the proposed NSFD scheme in conjunction with the trapezoidal rule, applied to the given test problems.

**Example 2.7.** Consider the second-order SPFIODE example

$$\begin{cases} -\epsilon y''(x) + (1 + \exp(x - 4)) y'(x) + y(x) + \frac{1}{2} \int_{0}^{1} y(s) ds = f(x), \\ y(0) = y(1) = 0. \end{cases}$$

The exact solution of Example 2.7 is  $y(x) = x - \left(\frac{e^{-\frac{(1-x)}{\epsilon}} - e^{\frac{-1}{\epsilon}}}{1-e^{\frac{-1}{\epsilon}}}\right)$ .



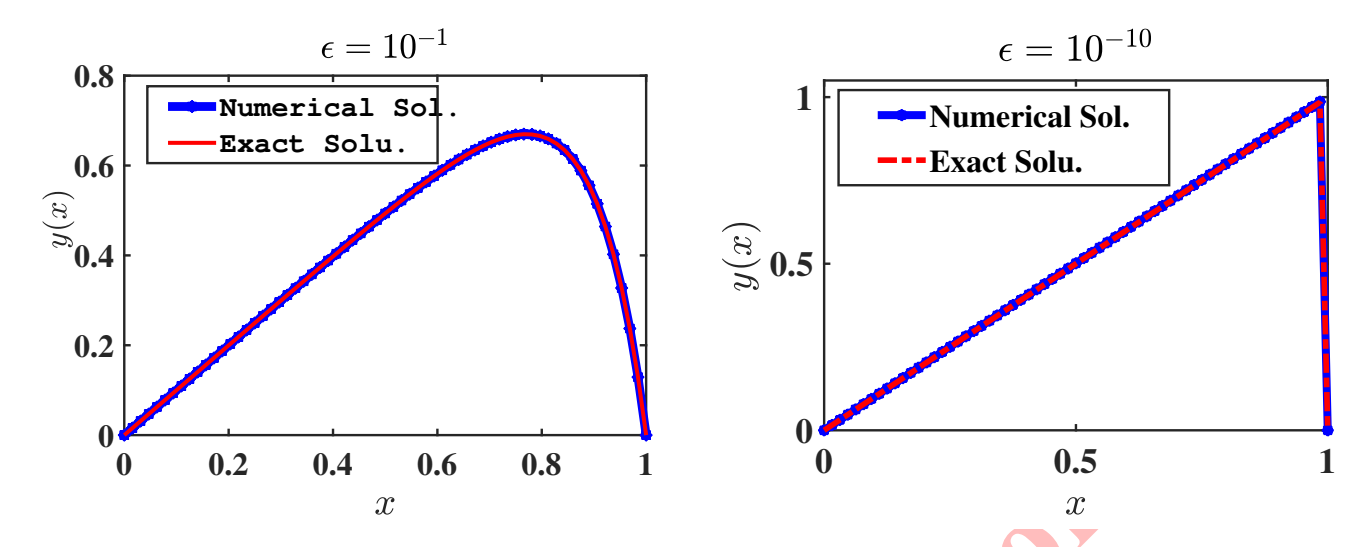


FIGURE 1. Numerical solution and exact solution of Example 2.7 for N=64.

Example 2.8. Consider the second-order SPFIODE example

$$\begin{cases} -\epsilon y''(x) + \left(1 - \frac{x^2}{2}\right)y'(x) + y + \frac{1}{4} \int_0^1 x \, y(s) \, ds = 1, \\ y(0) = y(1) = 0. \end{cases}$$

The maximum absolute error estimate for Example 2.7 is

$$e_{\epsilon}^{N} = \max_{0 < i < N} |y(x_i) - Y_i|,$$

and the converge rate is

$$p_{\epsilon}^{N} = \log_2\left(e_{\epsilon}^{N}/e_{\epsilon}^{2N}\right),$$

where  $y(x_i)$  is exact solution and  $Y_i$  is approximation solution.

Example 2.8 does not possess an exact solution. Consequently, an error estimate is followed by a double mesh error analysis. The maximum absolute error obtained by

$$e_{\epsilon}^{N} = \max_{0 < i < N} |y^{\epsilon, N} - \tilde{y}^{\epsilon, 2N}|,$$

where  $y^{\epsilon,N}$ ,  $\tilde{y}^{\epsilon,2N}$  are the approximate solutions of the related method with the mesh points N and 2N respectively. Now  $\epsilon$ -uniform pointwise maximum error  $E^N = \max_{\epsilon} e^N_{\epsilon}$  and also the parameter uniform convergence rate is  $P^N = \log_2\left(\frac{E^N}{E^{2N}}\right)$ .

For various values of  $\epsilon$ , a numerical and exact solution of Example 2.7 is plotted in Figure 1. The numerical solution of Example 2.8 with various  $\epsilon$  values is plotted in Figure 2. These figures show that when  $\epsilon$  decreases, a layer is presented around x=1. Tables 1 and 2 display Example 2.7 and Example 2.8 approximated maximum pointwise errors and rate of convergence respectively with various mesh points N. Table 3 compares the maximum absolute errors obtained using the standard finite difference method and the proposed NSFD scheme for Example 2.7.

### 3. Parabolic SPFIPDE

This section considers the singularly perturbed Fredholm integro-partial differential equation given in Equation (1.5). For small values of the perturbation parameter  $\epsilon$ , the solution u(x,t) typically exhibits a boundary layer near x=1.



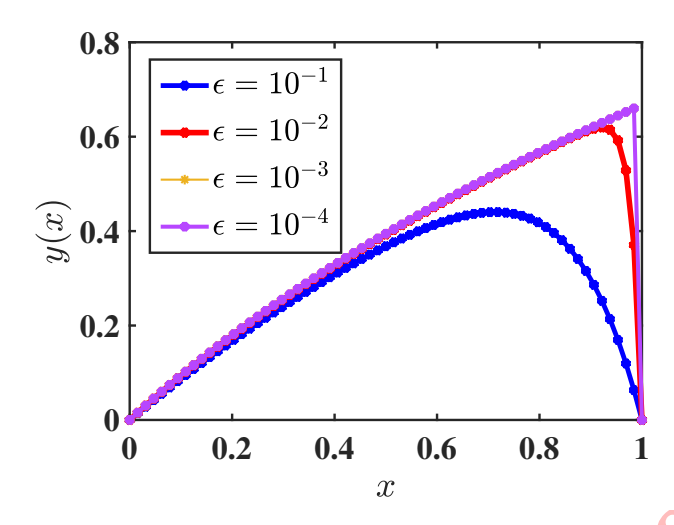


FIGURE 2. Solution plot of Example 2.8.

Table 1. Pointwise maximum error and convergence rate of Example 2.7.

$\epsilon\downarrow$	N = 64	128	256	512	1024
$10^{-2}$	5.0960e-4	1.6297e-4	6.4125e-5	2.9043e-5	1.3881e-5
	1.6447	1.3457	1.1427	1.0650	1.0298
$10^{-4}$	2.0055e-3	9.9520e-4	4.8585e-4	2.3013e-4	1.0196e-4
	1.0109	1.0345	1.0781	1.1744	1.2982
$10^{-6}$	2.0312e-3	1.0211e-3	5.1180e-4	2.5612e-4	1.2801e-4
	0.9922	0.9964	0.9988	1.0005	1.0025
$10^{-8}$	2.0315e-3	1.0213e-3	5.1206e-4	2.5638e-4	1.2827e-4
	0.9921	0.9961	0.9981	0.9990	0.9995
$10^{-10}$	2.0315e-3	1.0213e-3	5.1207e-4	2.5638e-4	1.2828e-4
	0.9921	0.9961	0.9980	0.9990	0.9995
$E^N$	2.0315e-3	1.0213e-3	5.1207e-4	2.5638e-4	1.2828e-4
$P^N$	0.9921	0.9960	0.9981	0.9990	

Table 2. Pointwise maximum error and convergence rate of Example 2.8.

$\epsilon\downarrow$	N = 64	128	256	512	1024
$10^{-2}$	1.7749e-3	1.0822e-3	6.0924e-4	3.2248e-4	1.6598e-4
<b>\</b>	0.7137	0.8289	0.9178	0.9582	0.9786
$10^{-4}$	9.5268e-4	4.8149e-4	2.4203e-4	1.2046e-4	5.6052e-5
	0.9845	0.9923	1.0066	1.1038	0.7923
$10^{-6}$	9.5268e-4	4.8149e-4	2.4204e-4	1.2135e-4	6.0755e-5
	0.9845	0.9922	0.9961	0.9981	0.9990
$10^{-8}$	9.5268e-4	4.8149e-4	2.4204e-4	1.2135e-4	6.0755e-5
	0.9845	0.9922	0.9961	0.9981	0.9990
$10^{-10}$	9.5268e-4	4.8149e-4	2.4204e-4	1.2135e-4	6.0755e-5
	0.9845	0.9922	0.9961	0.9981	0.9990
$E^N$	1.7749e-3	1.0822e-3	6.0924e-4	3.2248e-4	1.6598e-4
$P^N$	0.7138	0.8289	0.9178	0.9582	

To ensure smooth behavior at the corners (0,0) and (1,0), the following compatibility conditions are applied:

$$\begin{split} u_0(0) &= 0, \quad \text{and} \quad u_0(1) = 0, \\ &- \epsilon u_0''(0) + a(0,0)u_0'(0) + b(0,0)u_0(0) + \lambda \int_0^1 K(0,s)u_0(s) \, ds = f(0,0), \end{split}$$



TABLE 3. Maximum absolute errors comparison for standard and non-standard finite difference methods of Example 2.7.

$\epsilon$	N	Maximum absolute error	Maximum absolute	
		(Standard finite difference)	error (NSFD)	
	64	1.7684e-1	5.0960e-4	
	128	1.0392e-1	1.6297e-4	
$10^{-2}$	256	6.1874e-2	6.4125 e-5	
	512	3.3349e-2	2.9043e-5	
	1024	1.7339e-2	1.3881e-5	

$$-\epsilon u_0''(1) + a(1,0)u_0'(1) + b(1,0)u_0(1) + \lambda \int_0^1 K(1,s)u_0(s) \, ds = f(1,0).$$

Under these conditions, the solution satisfies the following estimates:

$$|u(x,t) - u_0(x)| \le Ct,$$

$$|u(x,t)| \le C(1-x) \quad \forall (x,t) \in \overline{Z}.$$
(3.1)

where C is a positive constant depending on the data, but independent of  $\epsilon$ . These bounds form the basis for the stability analysis.

**Lemma 3.1.** Assume  $a(x,t), f(x,t) \in C^{1,1}(\overline{Z}), \text{ and } \frac{\partial^n}{\partial x^n}K(x,s)$  exists and is continuous on  $[0,1] \times [0,1]$  for n=0,1. Further, suppose that  $|\lambda| < \frac{\alpha}{\Re}$ . Then the solution u(x,t) of Equation (1.5) satisfies the following bound:

$$|u_x(x,t)| \le C \left[ 1 + \epsilon^{-1} \exp\left(-\frac{\alpha(1-x)}{\epsilon}\right) \right], \quad \text{for all } (x,t) \in \overline{Z},$$

where C is a constant independent of  $\epsilon$ .

*Proof.* Fix any  $t \in [0,T]$  by using argument of Lemma 2.1 on the line segment  $\{(x,t)|0 \le x \le 1\}$ .

**Lemma 3.2.** If 
$$a(x,t), f(x,t) \in C^{1,1}(\overline{Z})$$
. Then  $|u_t(x,t)| < C$ , for  $(x,t) \in \overline{Z}$ .

*Proof.* One can find the proof of this lemma in [14]

**Lemma 3.3** (Stability). Assume that  $a(x,t), f(x,t) \in C^{4,2}(\overline{Z})$ , with a(x,t) = a(x) (i.e., independent of t). Let  $\frac{\partial^n}{\partial x^n}K(x,s) \in C([0,1] \times [0,1])$  for n=0,1,2,3,4, and suppose  $|\lambda| < \frac{\alpha}{\Re}$ . Then the solution u(x,t) of Equation (1.5) satisfies the following stability bounds:

$$|u(x,t)| \le C,$$

$$|u^{(i,j)}(x,t)| \le C \left[ 1 + \frac{1}{\epsilon^i} \exp\left( -\frac{\alpha(1-x)}{\epsilon} \right) \right], \quad \text{for } 0 \le i+j \le 4,$$
(3.2)

where  $u^{(i,j)} = \frac{\partial^{i+j} u}{\partial x^i \partial t^j}$ , and C is a constant independent of  $\epsilon$ .

*Proof.* By Equation (3.1),  $|u(x,t)| \leq Ct$ ,  $(x,t) \in \overline{Z}$ . Since  $t \in (0,T]$  therefore

$$|u(x,t)| \le C, \quad (x,t) \in \overline{Z}.$$

Proof of the Equation (3.2) using Lemma 3.1 and 3.2 and similar manner in [14, 26].



3.1. Numerical discretization for SPFPIDEs. In this section, the equation is first discretized in time using the backward Euler method. This time discretization results in a sequence of spatially dependent linear problems. To solve the spatial component at each time level, a fitted operator finite difference method is employed, while the integral term is approximated using the trapezoidal rule. The time interval [0, T] is uniformly partitioned as

$$\overline{\omega}^M = \{t_j = \tau j, \ 0 \le j \le M, \ \tau = \frac{T}{M}\}.$$

Then Equation (1.5) discretized on  $\overline{\omega}^M$ ,

$$\frac{u(x,t_j) - u(x,t_{j-1})}{\tau} + L_{\epsilon,x}(u(x,t_j)) + I_x(u(x,t_j)) = f(x,t_j), \ 1 \le j \le M,$$

$$u(x,0) = u_0, \ \forall \ x \in (0,1), \qquad u(0,t_j) = u(1,t_j) = 0.$$
(3.3)

To facilitate uniform convergence analysis, an auxiliary function  $\check{u}(x,t_j)$  is introduced. It satisfies the following equation:

$$\frac{\breve{u}(x,t_{j})-u(x,t_{j-1})}{\tau} + L_{\epsilon,x}(\breve{u}(x,t_{j})) + I_{x}(\breve{u}(x,t_{j})) = f(x,t_{j}), \ 1 \leq j \leq M,$$
 
$$\breve{u}(0,t_{j}) = \breve{u}(1,t_{j}) = 0.$$

This leads to the compact operator form:

$$(\mathcal{I} + \tau L_{\epsilon,x} + \tau I_x) \check{u}(x,t_i) = \tau f(x,t_i) + u(x,t_{i-1}). \tag{3.4}$$

where  $\check{u}(x,t_j)$  is the solution at time level  $t_j$  of this Equation (3.4). The local truncation error of the time semi-discretization of Equation (3.3) is defined by  $E_j = u(x,t_j) - \check{u}(x,t_j)$ .

In the temporal discretization, local error estimates at each time step contribute to the global error. The global error at time level  $t_i$  is denoted by  $e_i$ , where

$$e_j = \sum_{l=0}^{j} E_l, \quad j \le T/\tau.$$

Now, consider the integral term  $\int_{0}^{1} K(x,s)u(s,t)ds$ , where  $u(x,t) \in C^{4,2}[0,1]$  and  $K(x,s) \in C^{2}(\overline{Z})$ .

Let  $s_k = k(\Delta h)$ ,  $k = 0, 1, 2, \dots, N$  employing an analogous methodology as outlined in the Equation (2.3), then the composite trapezoidal rule is

$$\int_{0}^{1} K(x_{i}, s)u(s, t_{j}) ds \simeq T_{(\Delta h)}K(x_{i}, s)u(s, t_{j}) := (\Delta h) \left[ \frac{1}{2}K(x_{i}, s_{0})u(s_{0}, t_{j}) + K(x_{i}, s_{1})u(s_{1}, t_{j}) + \cdots + K(x_{i}, s_{N-1})u(s_{N-1}, t_{j}) + \frac{1}{2}K(x_{i}, s_{N})u(s_{N}, t_{j}) \right].$$

Let  $I_x U_i^j$  be the numerical discretization of the integral part in Equation (1.5). Then

$$I_x U_i^j = \lambda(\Delta h) \sum_{k=0}^N \theta_k K_i^k u_k^j$$
, where  $K_i^k = K(x_i, s_k)$ ,  $\theta_k = \begin{cases} \frac{1}{2}, & \text{for } k = 0, N, \\ 1, & \text{for } k = 1, 2, \dots, N-1. \end{cases}$ 

Next, construct a FOFD method to tackle this collection of linear equations. Consider the interval [0,1] with N subintervals, denoted as  $\overline{\varOmega}^N = \{x_i := i(\Delta h) \mid i = 0,1,\ldots,N\}$ , where  $\Delta h = \frac{1}{N}$  and let  $\overline{Z}^{N,M} = \overline{\varOmega}^N \times \overline{\omega}^M$  be the mesh of x,t variables and  $Z^{N,M} = \overline{Z}^{N,M} \cap Z$ .

Now applying Mickens' theory [21] of difference equations and building the following scheme:

$$L_{\epsilon,x}^{N,M}U_i^j = \frac{U_i^j - U_i^{j-1}}{\tau} + L_{\epsilon,x}^N U_i^j + I_x U_i^j = f_i^j, \tag{3.5}$$



where

$$L_{\epsilon,x}^{N}U_{i}^{j} = -\epsilon \left[ \frac{U_{i+1}^{j} - 2U_{i}^{j} + U_{i-1}^{j}}{\phi_{i}^{2}} \right] + a_{i}^{j} \frac{U_{i}^{j} - U_{i-1}^{j}}{\Delta h} + b_{i}^{j}U_{i}^{j},$$

here

$$\phi_i^2 = \frac{\epsilon(\Delta h)}{a_i^j} \left( \exp\left(\frac{a_i^j(\Delta h)}{\epsilon}\right) - 1 \right).$$

Now the Equation (3.5) becomes

$$L_{\epsilon,x}^{N,M} U_i^j = \frac{U_i^j - U_i^{j-1}}{\tau} - \epsilon \left[ \frac{U_{i+1}^j - 2U_i^j + U_{i-1}^j}{\phi_i^2} \right] + a_i^j \frac{U_i^j - U_{i-1}^j}{\Delta h} + b_i^j U_i^j$$

$$+ \lambda(\Delta h) \sum_{k=0}^N \theta_k K_i^k u_k^j, \quad \text{where} \quad \theta_k = \begin{cases} \frac{1}{2}, & \text{for } k = 0, N, \\ 1, & \text{for } k = 1, 2, \cdots, N-1, \end{cases}$$
screte initial and boundary conditions
$$U_i^0 = u_0(x_i), \ i = 0, 1, \cdots, N,$$
(3.6)

with discrete initial and boundary conditions

$$U_i^0 = u_0(x_i), i = 0, 1, \dots, N,$$
  
 $U_0^j = U_N^j = 0, 1 < j < M,$ 

The Equation (3.6) is a linear system equation AU = b. Solving the linear system (3.6) is given in Algorithm 2.

## Algorithm 2 Numerical Solution of parabolic SPFIPDE

- 1: function solve\_linear\_system(A, b)
- 2: **Input:**  $A = a[i, j], U = u_i, b = f_i + u[i, j 1](1/\tau)$
- 3: Initial\_condition:  $u[i,0] = u_0$
- 4: boundary\_conditions: u[0,j]=u[N,j]=0
- 5: **for** j = 1 **to** M **do**
- $U \leftarrow A \backslash b$
- return U
- 8: end for
- 9:  $\mathbf{Output:}$   $\mathbf{numerical\_solution}$  U
- 3.2. Error analysis for SPFPIDEs. If  $u_{D_t}(x_i, t_j), u_{D_x}(x_i, t_j), u_I(x_i, t_j)$  be the continuous solution of time derivative, spatial derivative and integral part respectively and  $(U_{D_t})_i^j, (U_{D_r})_i^j, (U_I)_i^j$  be the numerical solution of time derivative, spatial derivative and integral part respectively.

**Lemma 3.4.** The local error  $E_j = u_{D_t}(x_i, t_j) - (U_{D_t})_i^j$  associated with the Equation (3.3) satisfies

$$||E_j||_{\infty} \le C\tau^2, \ 1 \le j \le M.$$

*Proof.* The proof can be found in [9].

**Theorem 3.5.** The global error  $e_j = \sum_{l=0}^{j} E_l$  is estimate with (3.3), its satisfies

$$||e_i||_{\infty} \leq C\tau, \ 1 \leq j \leq M.$$

*Proof.* One can find the proof of this theorem in [9].



**Theorem 3.6.** Let  $u(x_i, t_j)$  be the continuous solution for the differential part of (3.3) and  $U_i^j$  be the numerical solution for the differential part of (3.6) both at time level j. Then

$$\sup_{0 < \epsilon < 1} \max_{\substack{0 \le i \le N \\ 0 \le j \le M}} |u_{D_x}(x_i, t_j) - (U_{D_x})_i^j| \le C(\Delta h).$$

where C is an independent constant of  $\epsilon$  and  $\Delta h$ .

*Proof.* As a consequence, the temporal discretization is uniformly convergent in the first order. Keeping things simple, leave out the time level index temporarily.

$$L_{\epsilon}^{N}((u_{D_{x}})_{i} - (U_{D_{x}})_{i}) = (L_{\epsilon,x} - L_{\epsilon,x}^{N})u_{i},$$

$$= -\epsilon u_{i}'' + a_{i}u_{i}' + \left[\epsilon \frac{u_{i+1} - 2u_{i} + u_{i-1}}{\phi_{i}^{2}((\Delta h), \epsilon, t)}\right] - a_{i}\left[\frac{u_{i} - u_{i-1}}{\Delta h}\right].$$
(3.7)

Using proper Taylor series expansions and considering the truncated Taylor expansion  $\frac{1}{\phi_i^2} = \frac{1}{(\Delta h)^2} - \frac{a_i}{2\epsilon(\Delta h)} + \frac{a_i^2}{12\epsilon^2}$ . Then the Equation (3.7) becomes,

$$\begin{split} L_{\epsilon}^{N}\left((u_{D_{x}})_{i}-(U_{D_{x}})_{i}\right) &= -\epsilon u_{i}'' + \left[\left(\frac{\epsilon}{(\Delta h)^{2}} - \frac{a_{i}}{2(\Delta h)} + \frac{a_{i}^{2}}{12\epsilon}\right)\left((\Delta h)^{2}u_{i}'' + \frac{(\Delta h)^{4}}{12}u_{i}'''(\eta_{i})\right)\right] + \frac{a_{i}(\Delta h)}{2}u_{i}'', \\ \left|L_{\epsilon}^{N}\left((u_{D_{x}})_{i}-(U_{D_{x}})_{i}\right)\right| &= \left|\epsilon\frac{(\Delta h)^{2}}{12}u_{i}''''(\eta_{i})\right| + \left|\frac{a_{i}(\Delta h)}{2}u_{i}''\right| + \left|\frac{a_{i}(\Delta h)^{3}}{24}u_{i}''''(\eta_{i})\right| + \left|\frac{a_{i}^{2}(\Delta h)^{2}}{12\epsilon}u_{i}''\right| \\ &+ \left|\frac{a_{i}^{2}(\Delta h)^{4}}{144\epsilon}u_{i}''''(\eta_{i})\right| + \left|\frac{a_{i}(\Delta h)}{2}u_{i}''\right|, \quad \text{where} \quad \eta_{i} \in (x_{i+1}, x_{i-1}), \end{split}$$

using  $\Delta h > (\Delta h)^2 > (\Delta h)^4$  relation and also using Lemma 2.2 and 3.3, then

$$|L_{\epsilon}^{N}\left((u_{D_{x}})_{i}-(U_{D_{x}})_{i}\right)|\leq C(\Delta h).$$

Restoring the time level index, we obtain:

ng the time level index, we obtain: 
$$|L_{\epsilon}^{N,M}\left(\left(u_{D_{x}}\right)_{i}^{j}-\left(U_{D_{x}}\right)_{i}^{j}\right)|\leq C(\Delta h).$$
 we the proof of this theorem.

It follows the proof of this theorem.

**Lemma 3.7.** If  $u_I(x_i,t_j)$  is the integral part continuous solution and  $(U^I)_i^j$  is the numerical solution of the integral part. Then the composite trapezoidal rule has a convergence order of two

$$\sup_{0 \le i \le N} |U_I(x_i, t_j) - (U^I)_i^j| \le C(\Delta h)^2,$$

where C is an independent constant of  $\Delta h$ .

*Proof.* using the technique of Lemma 2.4, the theorem follows.

$$\int_{0}^{1} K(x_{i}, s)u(s, t_{j}) ds - T_{(\Delta h)}K(x_{i}, s)u(s, t_{j}) = \frac{-1}{12} (\Delta h)^{2} \left| \frac{\partial^{2}}{\partial \xi^{2}} K(x_{i}, \xi)u(\xi, t_{j}) \right|, \ \xi \in [0, 1],$$

apply Lemma 2.5 in a similar manner the rate of convergence of the composite trapezoidal rule is two.

**Theorem 3.8.** Let u(x,t) be the continuous solution and  $U_i^j$  be the numerical solution of Equation (1.5). Then

$$\sup_{0<\epsilon<1} \max_{\substack{0\leq i\leq N\\0\leq j\leq M}} \left|u_i^j-U_i^j\right| \leq C(\Delta h + \tau).$$

where C is an independent constant of  $\epsilon$ ,  $\tau$  and  $\Delta h$ .



Proof. Using Theorems 3.5, 3.6 and Lemma 3.7 then error bound is

$$\begin{aligned} |u_i^j - U_i^j| &= |(u_{D_t}(x_i, t_j) + u_{D_x}(x_i, t_j) + u_I(x_i, t_j)) - ((U_{D_t})_i^j + (U_{D_x})_i^j + (U_I)_i^j)|, \\ &\leq |u_{D_t}(x_i, t_j) - (U_{D_t})_i^j| + |u_{D_x}(x_i, t_j) - (U_{D_x})_i^j| + |u_I(x_i, t_j) - (U_I)_i^j|, \\ &\leq C\tau + C(\Delta h) + C(\Delta h)^2, \\ &< C(\Delta h + \tau). \end{aligned}$$

3.3. Numerical calculation for SPFPIDEs. Theoretical research indicates that independent of the perturbation parameter  $\epsilon$ , the devised approach shows a uniform convergence rate of order one in time and space. The numerical approach and results for three test problems are shown below.

Example 3.9. Consider the SPFPIDE example

$$\begin{cases} \frac{\partial u(x,t)}{\partial t} - \epsilon \frac{\partial^2 u(x,t)}{\partial x^2} + \frac{\partial u(x,t)}{\partial x} + \int_0^1 u(s,t) \, ds = f(x,t), & (x,t) \in \mathbb{Z}, \\ u(x,0) = u_0, & u(0,t) = u(1,t) = 0. \end{cases}$$

The exact solution of Example 3.9 is  $u(x,t) = e^{-t} \left[ e^{\frac{-1}{\epsilon}} + x \left( 1 - e^{\frac{-1}{\epsilon}} \right) - e^{-\frac{(1-x)}{\epsilon}} \right]$ .

Example 3.10. Consider the SPFPIDE example

$$\begin{cases} \frac{\partial u(x,t)}{\partial t} - \epsilon \frac{\partial^2 u(x,t)}{\partial x^2} + 2 \frac{\partial u(x,t)}{\partial x} + (1+x) u(x,t) + \int_0^1 u(s,t) \, ds = f(x,t), & (x,t) \in \mathbb{Z}, \\ u(x,0) = u_0, & u(0,t) = u(1,t) = 0. \end{cases}$$

The exact solution of Example 3.10 is  $u(x,t) = e^{-t} \left[ e^{\frac{-2}{\epsilon}} + e^{-2\frac{(1-x)}{\epsilon}} - x \right].$ 

Example 3.11. Consider the SPFPIDE example

$$\begin{cases} \frac{\partial u(x,t)}{\partial t} - \epsilon \frac{\partial^2 u(x,t)}{\partial x^2} + (2+x^2) \frac{\partial u(x,t)}{\partial x} + u(x,t) + \int\limits_0^1 (x+1)u(s,t) \, ds = t^3, & (x,t) \in \mathbb{Z}, \\ u(x,0) = u(0,t) = u(1,t) = 0. \end{cases}$$

The maximum absolute error estimate of Example 3.9 and 3.10 are

$$e_{\epsilon}^{N,\tau} = |u(x_i, t_j) - U_i^j|,$$

and the computed  $\epsilon$ -uniform pointwise maximum error  $E^{N,\tau} = \max_{\epsilon} e_{\epsilon}^{N,\tau}$ , where  $u(x_i, t_j)$  is the exact solution and  $U_i^j$  is the approximation solution. The computed parameter rate of uniform convergence is defined by

$$p^{N,\tau} = \log_2\left(\frac{e^{N,\tau}}{e^{2N,\frac{\tau}{2}}}\right).$$

and the maximum order of convergence is given by  $P^{N,\tau} = \log_2\left(\frac{E^{N,\tau}}{E^{2N,\frac{\tau}{2}}}\right)$ .

In Example 3.11 the exact solution is unknown. Therefore, a double mesh approach and a modified version of a double mesh concept to assess the error in the computed approximations

$$e^{N,\tau}_{\epsilon} = \max_{0 \leq i \leq N, 0 \leq j \leq M} \left| U^{i,j}_{\epsilon,N,\tau} - U^{i,j}_{\epsilon,2N,\frac{\tau}{2}} \right|,$$



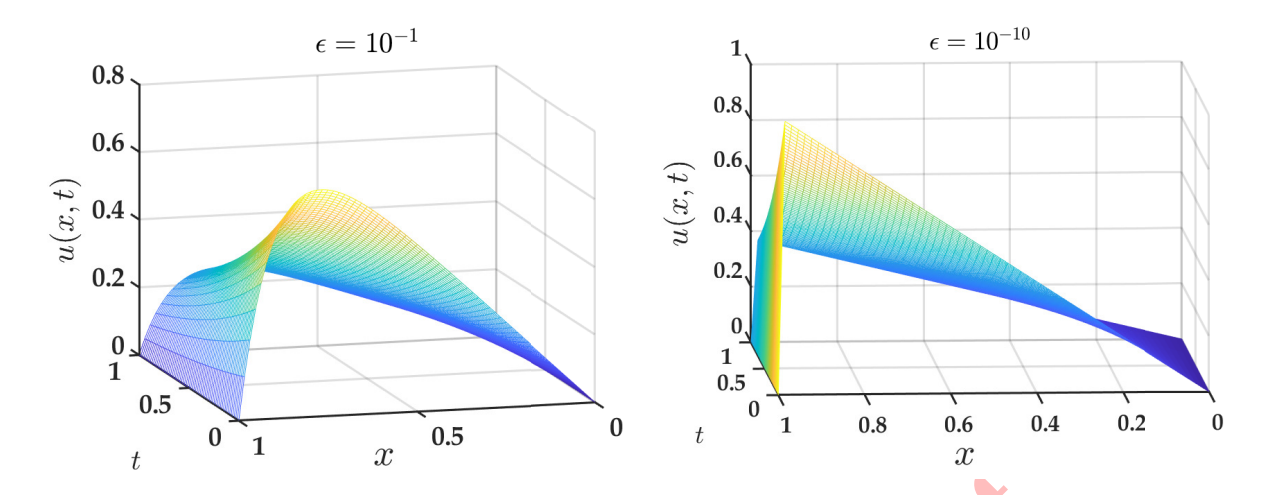


FIGURE 3. Surface plots of numerical solution of Example 3.9 for N = 64.

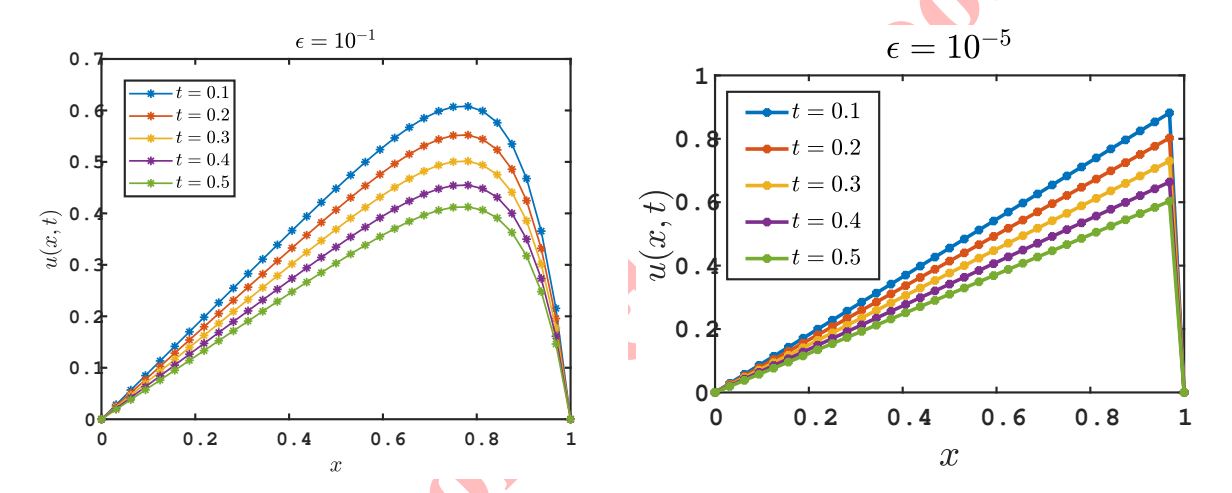


FIGURE 4. Solution plots of Example 3.9 with corresponding values of  $\epsilon$ .

where  $U^{i,j}_{\epsilon,N,\tau}$  is the approximation solution with N mesh points and time step  $\tau$ . In the same way  $U^{i,j}_{\epsilon,2N,\frac{\tau}{2}}$  is the approximation solution with 2N mesh points and  $\tau/2$  time step.

Surface plots for  $\epsilon = 10^{-1}$  and  $\epsilon = 10^{-10}$  are shown in Figures 3, 6, and 9 for Examples 3.9, 3.10, and 3.11, respectively, on a uniform mesh. Figures 4 and 7 display the solutions for  $\epsilon = 10^{-1}$  and  $\epsilon = 10^{-5}$  for Examples 3.9 and 3.10, while Figure 10 shows the solutions for  $\epsilon = 10^{-1}$  and  $\epsilon = 10^{-10}$  for Example 3.11 at different time levels. Figures 5, 8, and 11 display the solution for different values of  $\epsilon$  at fixed time levels t = 0.5 and t = 1 for Examples 3.9, 3.10, and 3.11, respectively. These results indicate the presence of boundary layers near x = 1. Figures 12(a) and 12(b) present the numerical convergence rates on a log-log scale, providing a graphical representation of the method's performance. Furthermore, Table 4, Table 5 and Table 6 display the maximum pointwise error and rate of convergence of order one for Example 3.9, Example 3.10 and Example 3.11. Table 7 presents a comparison of the maximum absolute errors between the standard finite difference and the NSFD methods for Example 3.9. As shown, the NSFD method is specifically designed to handle singular perturbations and accurately resolve sharp boundary layers. By using fitted meshes or specially constructed denominator functions, NSFD ensures stability and uniform convergence even for very small values of  $\epsilon$ . Although it involves a more complex, problem-specific implementation, the NSFD method consistently delivers greater accuracy and reliability compared to standard finite difference schemes.



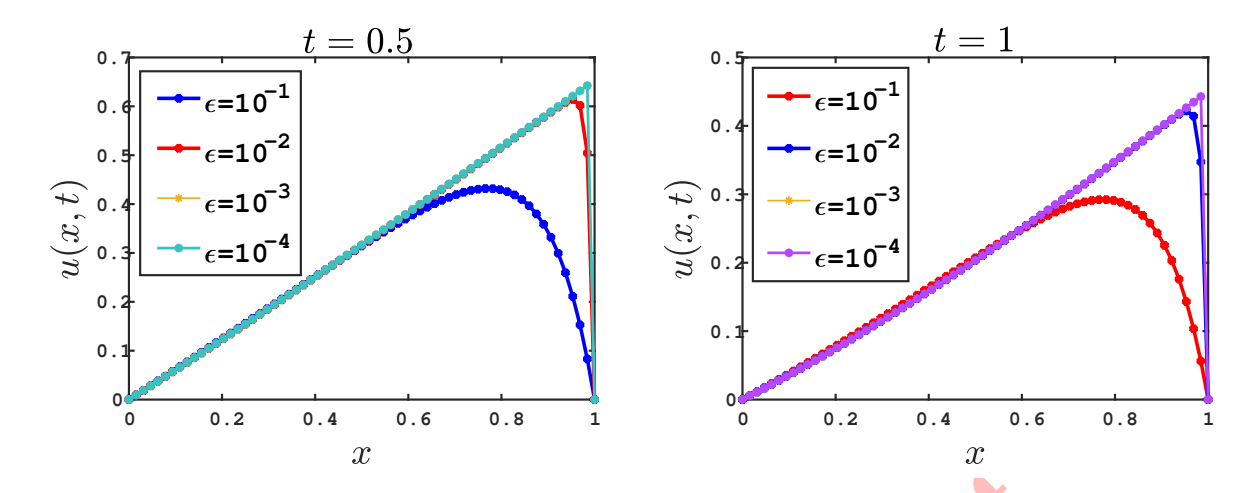


FIGURE 5. Solution plots of Example 3.9 with corresponding values of t.

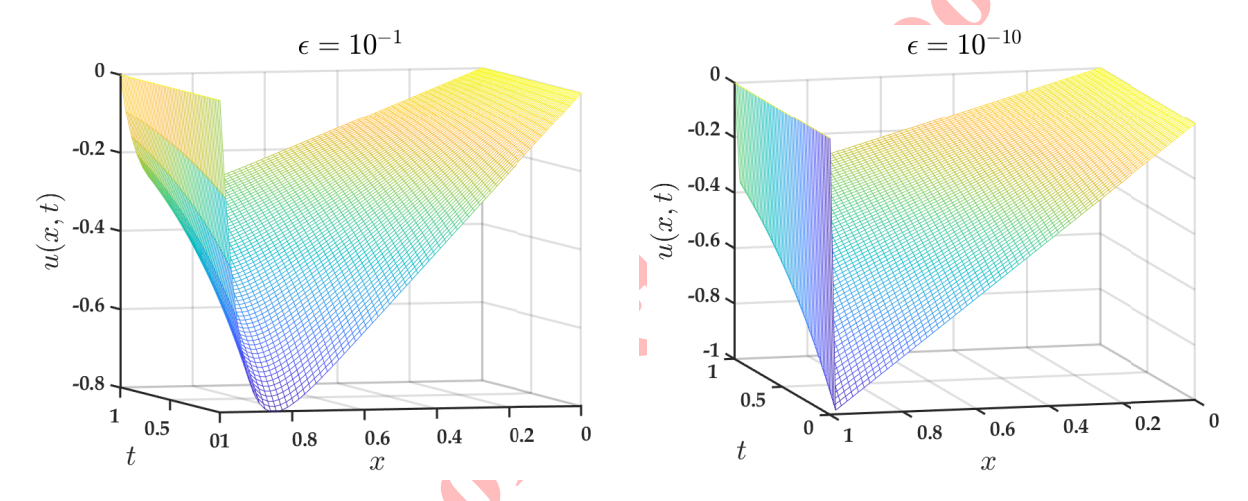


FIGURE 6. Surface plots of numerical solution of Example 3.10 for N=64.

The general workflow for this article is illustrated in the flowchart below in Figure 13.

## 4. Conculsion

This research aimed to determine the maximum pointwise error and the convergence rate for the numerical computations of SPFIODEs and SPFIPDEs. A significant use of the current methodologies, which nearly achieve first-order convergence rates in both spatial and temporal directions. Our methodology employed a non-standard finite difference scheme for spatial derivatives, the composite trapezoidal rule for integral components with a uniform mesh, and the backward Euler method for time derivatives on uniform meshes in SPFIPDEs. Approaching singularly perturbed integro-differential equations with a tiny independent parameter and attaining first-order convergence rates in both spatial and temporal directions represent significant novelty in this area of research. The significant discoveries and contributions of our studies are:

- Understanding boundary layer processes in the solution using a uniform spatial mesh.
- The effective utilization of the non-standard finite difference approach for spatial derivatives with a small parameter  $\epsilon$ .



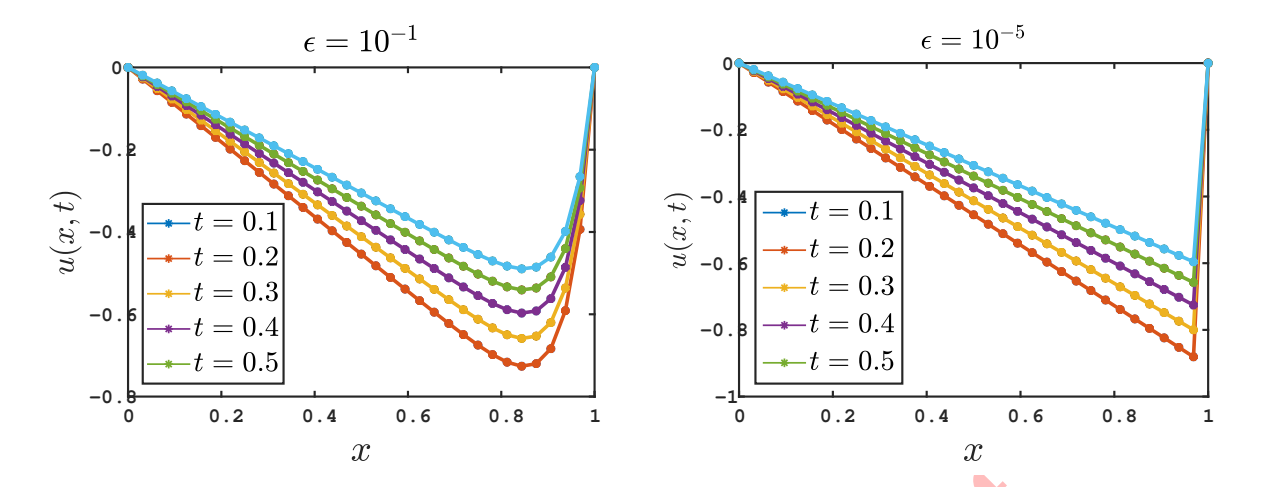


FIGURE 7. Solution plots of Example 3.10 with corresponding values of  $\epsilon$ .

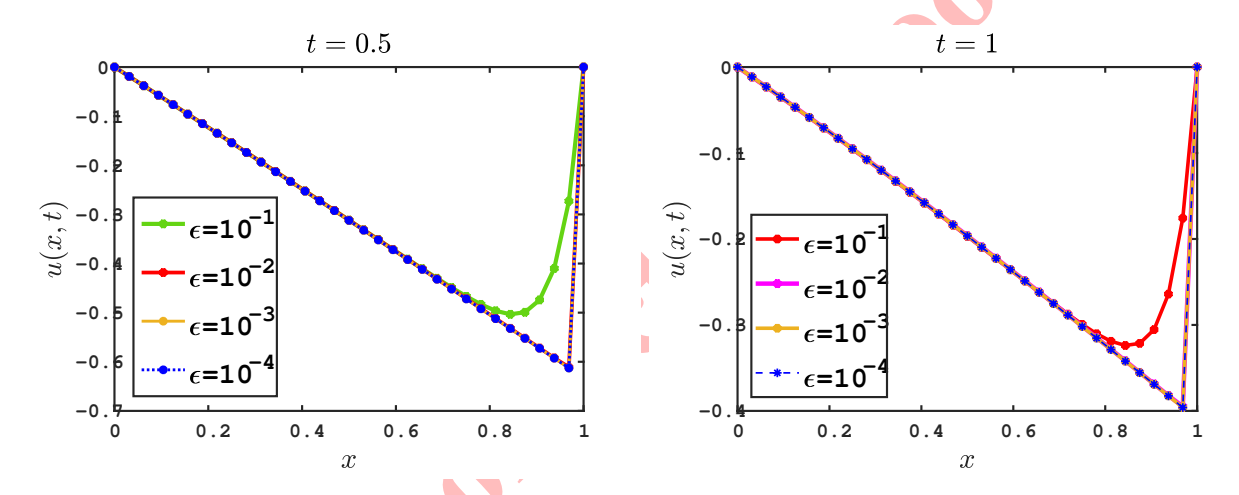


FIGURE 8. Solution plots of Example 3.10 with corresponding values of t.

• Achievement of first-order convergence rates for both SPFIODEs and SPFIPDEs, representing a significant improvement over previous efforts.

## ACKNOWLEDGMENT

# Availability of supporting data

Not applicable.

# **Funding**

Not applicable.

# Ethical approval



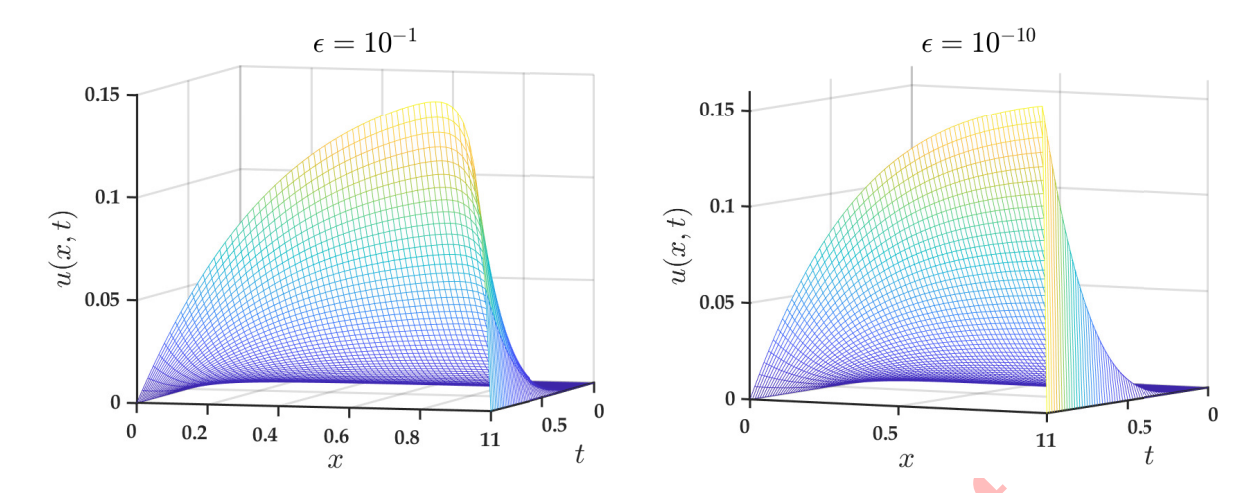


FIGURE 9. Surface plots of numerical solution of Example 3.11 for N = 64.

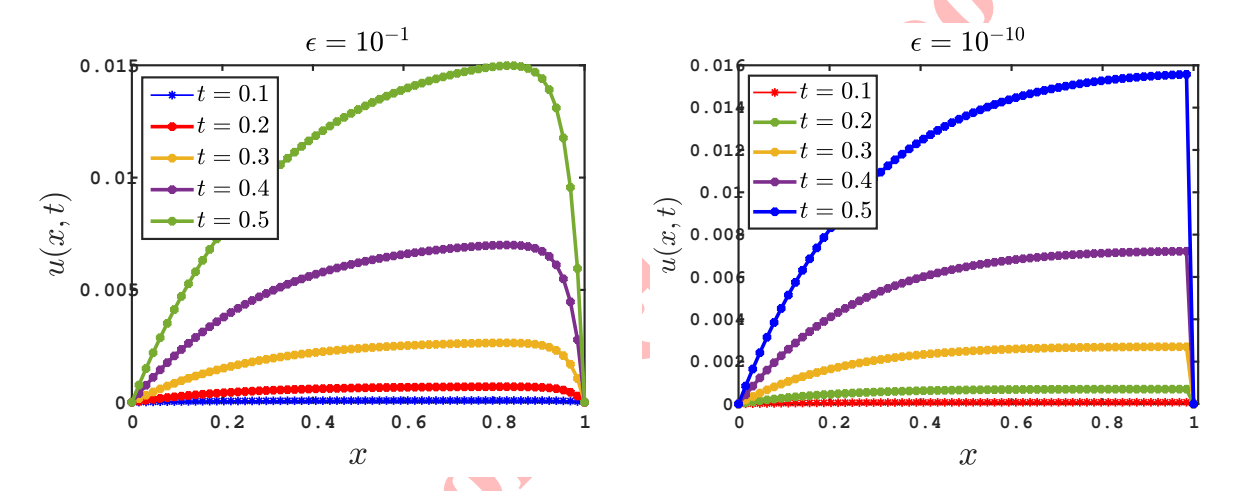


FIGURE 10. Solution plots of Example 3.11 with corresponding values of t.

Not applicable.

# Declaration of competing interest

The authors declare that they have no competing interests concerning the publication of the manuscript.



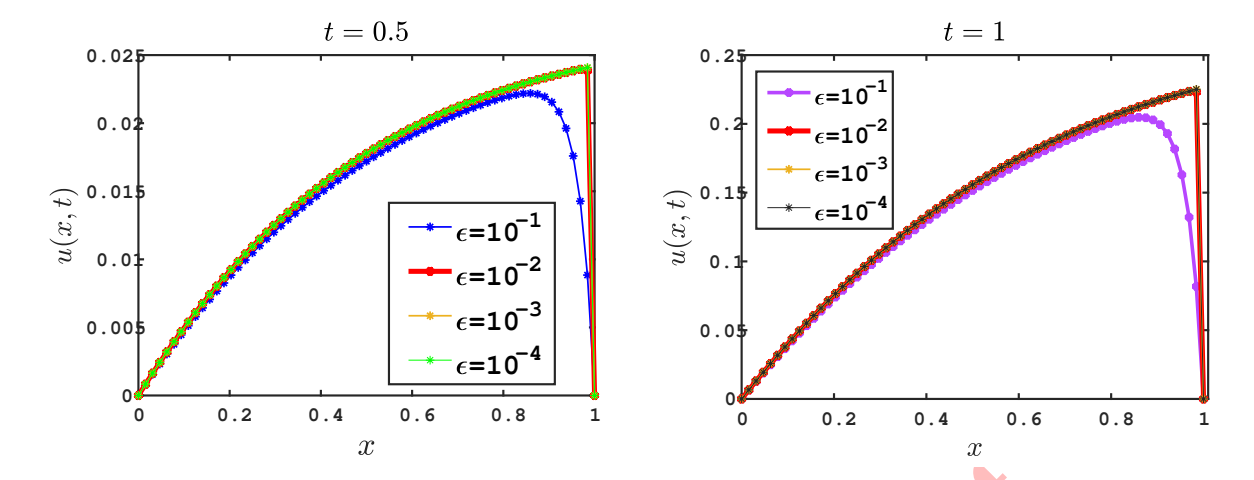


Figure 11. Solution plots of Example 3.11 with corresponding values of  $\epsilon$ .

Table 4. Pointwise maximum error and convergence rate of Example 3.9.

	Number of intervals N and $\tau = \frac{1}{N}$				
$\epsilon\downarrow$	64	128	256	512	1024
$10^{-2}$	2.5367e-3	1.1060e-3	5.1111e-4	2.4493e-4	1.1981e-4
	1.1975	1.1137	1.0613	1.0316	1.0160
$10^{-4}$	4.9148e-3	2.4879e-3	1.2356e-3	5.9940e-4	2.7926e-4
	0.9822	1.0097	1.0436	1.1019	1.2104
$10^{-6}$	4.9540e-3	2.5283e-3	1.2769e-3	6.4113e-4	3.2092e-4
	0.9704	0.9856	0.9939	0.9984	1.0009
$10^{-8}$	4.9544e-3	2.5287e-3	1.2773e-3	6.4155e-4	3.2134e-4
	0.9703	0.9853	0.9934	0.9975	0.9990
$10^{-10}$	4.9544e-3	2.5287e-3	1.2773e-3	6.4155e-4	3.2134e-4
	0.9703	0.9853	0.9934	0.9974	0.9990
$E^{N,\tau}$	4.9544e-3	2.5287e-3	1.2773e-3	6.4155e-4	3.2134e-4
$P^{N,\tau}$	0.9703	0.9853	0.9935	0.9975	

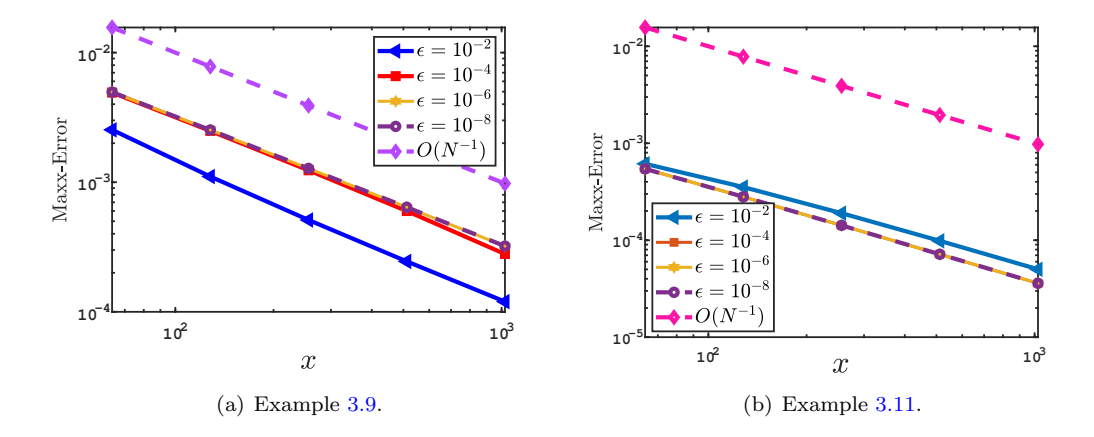


FIGURE 12. Log-log plot with corresponding values of  $\epsilon$ .



Table 5. Pointwise maximum error and convergence rate of Example 3.10.

	Number of intervals $N$ and $\tau = \frac{1}{N}$				
$\epsilon\downarrow$	64	128	256	512	1024
$10^{-2}$	1.6464e-3	6.7875e-4	2.9506e-4	1.3597e-4	6.5069e-5
	1.2784	1.2019	1.1177	1.0633	1.0326
$10^{-4}$	2.5166e-3	1.2827e-3	6.4472e-4	3.1950e-4	1.5507e-4
	0.9723	0.9924	1.0128	1.0429	1.1005
$10^{-6}$	2.5265e-3	1.2929e-3	6.5510e-4	3.3002e-4	1.6569e-4
	0.9665	0.9808	0.9891	0.9941	0.9973
$10^{-8}$	2.5266e-3	1.2930e-3	6.5520e-4	3.3013e-4	1.6579e-4
	0.9665	0.9807	0.9889	0.9936	0.9964
$10^{-10}$	2.5266e-3	1.2930e-3	6.5520e-4	3.3013e-4	1.6579e-4
	0.9665	0.9807	0.9889	0.9936	0.9963
$E^{N,\tau}$	2.5266e-3	1.2930e-3	6.5520e-4	3.3013e-4	1.6579e-4
$P^{N,\tau}$	0.9665	0.9807	0.9889	0.9937	

Table 6. Pointwise maximum error and convergence rate of Example 3.11.

	Number of intervals N and $\tau = \frac{1}{N}$				
$\epsilon\downarrow$	64	128	256	512	1024
$10^{-2}$	6.1340e-4	3.5310e-4	1.8993e-4	9.8452e-5	5.0109e-5
	0.7968	0.8946	0.9480	0.9744	0.9873
$10^{-4}$	5.4388e-4	2.8011e-4	1.4212e-4	7.1581e-5	3.5922e-5
	0.9573	0.9789	0.9895	0.9947	0.9898
$10^{-6}$	5.4388e-4	2.8011e-4	1.4212e-4	7.1581e-5	3.5921e-5
	0.9573	0.9789	0.9895	0.9947	0.9974
$10^{-8}$	5.4388e-4	2.8011e-4	1.4212e-4	7.1581e-5	3.5921e-5
	0.9573	0.9789	0.9895	0.9947	0.9974
$10^{-10}$	5.4388e-4	2.8011e-4	1.4212e-4	7.1581e-5	3.5921e-5
	0.9573	0.9789	0.9895	0.9947	0.9974
$E^{N,\tau}$	6.5193e-4	3.5310e-4	1.8993e-4	9.8452e-5	5.0109e-5
$P^{N,\tau}$	0.8846	0.8946	0.9480	0.9744	

TABLE 7. Maximum absolute errors comparison for standard and non-standard finite difference methods of Example 3.9,

$\epsilon$ N and	$N$ and $\tau = \frac{1}{N}$	Maximum absolute error	Maximum absolute
	$N \text{ and } T = \overline{N}$	(standard finite difference)	error (NSFD)
	64	1.5849e-1	2.5367e-3
	128	9.4261e-2	1.1060e-3
$10^{-2}$	$\begin{array}{c c} 10^{-2} & 256 \\ 512 &  \end{array}$	5.6225e-2	5.1111e-4
		3.0303e-2	2.4493e-4
	1024	1.5779e-2	1.1981e-4



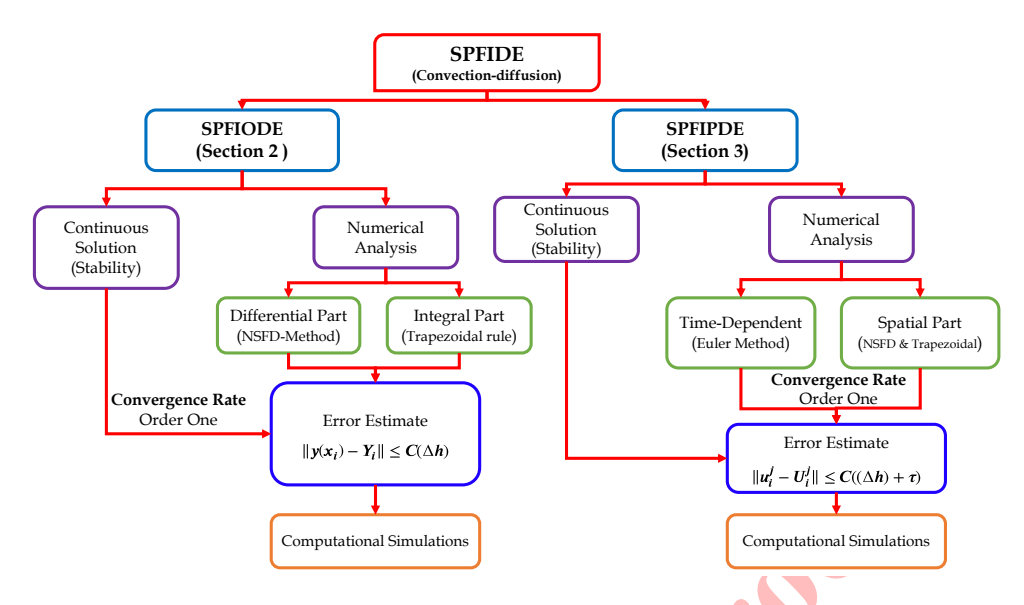


FIGURE 13. Workflow chart

## References

- [1] M. Abbaszadeh, M. Dehghan, and Y. Zhou, Crank-Nicolson/Galerkin spectral method for solving two-dimensional time-space distributed-order weakly singular integro-partial differential equation, J. Comput. Appl. Math., 374(3) (2020), 112739.
- [2] M. Abbaszadeh and M. Dehghan, A finite-difference procedure to solve weakly singular integro partial differential equation with space-time fractional derivatives, Eng. Comput., 37(9) (2021), 2173–2182.
- [3] A. Akyuz-Dascioglu and M. Sezer, A Taylor polynomial approach for solving the most general linear Fredholm integro-differential-difference equations, Math. Methods Appl. Sci., 35(7) (2012), 839–844.
- [4] G. M. Amiraliyev, M. E. Durmaz, and M. Kudu, Fitted second-order numerical method for a singularly perturbed Fredholm integro-differential equation, Bull. Belg. Math. Soc. Simon Stevin, 27(1) (2020), 71–88.
- [5] G. M. Amiraliyev, M. E. Durmaz, and M. Kudu, Uniform convergence results for singularly perturbed Fredholm integro-differential equation, J. Math. Anal., 6 (2018), 55–64.
- [6] S. Bala, L. Govindarao, A. Das, and A. Majumdar, Numerical scheme for partial differential equations involving small diffusion term with non-local boundary conditions, J. Appl. Math. Comput., 69 (2023), 4307–4331.
- [7] J. Chen, Y. Huang, H. Rong, T. Wu, and T. Zeng, A multiscale Galerkin method for second-order boundary value problems of Fredholm integro-differential equation, J. Comput. Appl. Math., 290 (2015), 633–640.
- [8] E. Cimen and M. Cakir, A uniform numerical method for solving singularly perturbed Fredholm integro-differential problem, Comput. Appl. Math., 40 (2021), 42.
- [9] C. Clavero, J. C. Jorge, and F. Lisbona, A uniformly convergent scheme on a nonuniform mesh for convection diffusion parabolic problems, J. Comput. Appl. Math., 154(2) (2003), 415–429.
- [10] M. E. Durmaz and G. M. Amiraliyev, A robust numerical method for a singularly perturbed Fredholm integrodifferential equation, Mediterr. J. Math., 18(24) (2021), 24.
- [11] L. Govindarao and J. Mohapatra, A second-order weighted numerical scheme on nonuniform meshes for convection diffusion parabolic problems, Eur. J. Comput. Mech., 28(5) (2019), 467–497.
- [12] L. Govindarao, H. Ramos, and S. Elango, Numerical scheme for singularly perturbed Fredholm integro-differential equations with non-local boundary conditions, Comput. Appl. Math., 43 (2024), 126.
- [13] L. Govindarao and E. Sekar, B-spline method for second order RLC closed series circuit with small inductance value, J. Phys. Conf. Ser., 2646 (2023), 012039.



REFERENCES 23

[14] M. K. Kadalbajoo and A. Awasthi, A parameter uniform difference scheme for singularly perturbed parabolic problem in one space dimension, Appl. Math. Comput., 183 (2006), 42–60.

- [15] M. K. Kadalbajoo, A. Kumar, and L. P. Tripathi, A radial basis function based implicit-explicit method for option pricing under jump-diffusion models, Appl. Numer. Math., 110 (2016), 159–173.
- [16] R. B. Kellogg and A. Tsan, Analysis of some difference approximations for a singular perturbation problem without turning points, Math. Comput., 32(144) (1978), 1025–1039.
- [17] R. Kress, Numerical Analysis, Springer, New York, 1998.
- [18] C. G. Lange and D. R. Smith, Singular perturbation analysis of integral equations, Stud. Appl. Math., 90(1) (1993), 1–74.
- [19] S. Li, G. I. Shishkin, and L. P. Shishkina, Approximation of the solution and its derivative for the singularly perturbed Black-Scholes equation with nonsmooth initial data, Comput. Math. Math. Phys., 47 (2007), 442–462.
- [20] N. A. Mbroh and J. B. Munyakazi, A fitted operator finite difference method of lines for singularly perturbed parabolic convection-diffusion problems, Math. Comput. Simul., 165 (2019), 156–171.
- [21] R. E. Mickens, Nonstandard Finite Difference Models of Differential Equations, World Scientific, Singapore, 1994.
- [22] J. J. H. Miller, E. O'Riordan, and G. I. Shishkin, Fitted Numerical Methods for Singular Perturbation Problems, World Scientific, Singapore, 1996.
- [23] J. Mohapatra, L. Govindarao, and S. Priyadarshana, A splitting based higher-order numerical scheme for 2D time-dependent singularly perturbed reaction-diffusion problems, J. Supercomput., 81(1) (2025), 203.
- [24] J. Mohapatra, S. Priyadarshana, and N. R. Reddy, Uniformly convergent computational method for singularly perturbed time delayed parabolic differential-difference equations, Eng. Comput., 40(1) (2023), 694–717.
- [25] J. B. Munyakazi and K. C. Patidar, Limitations of Richardson's extrapolation for a high order fitted mesh method for self-adjoint singularly perturbed problems, J. Appl. Math. Comput., 32 (2010), 219–236.
- [26] M. J. Ng-Stynes, E. O'Riordan, and M. Stynes, Numerical methods for time-dependent convection diffusion equations, J. Comput. Appl. Math., 21(3) (1988), 28-310.
- [27] K. C. Patidar, High order fitted operator numerical method for self-adjoint singular perturbation problems, Appl. Math. Comput., 171(1) (2005), 547–566.
- [28] P. A. Prince, L. Govindarao, and S. Elango, Non-standard finite difference scheme for system of singularly perturbed Fredholm integro-differential equations, J. Math. Model., 13(4) (2025), 865-882.
- [29] S. Priyadarshana, Monotone hybrid numerical method for singularly perturbed time-lagged semilinear parabolic problems, Natl. Acad. Sci. Lett., 46(16) (2023), 347–350.
- [30] S. Priyadarshana and J. Mohapatra, An efficient fractional step numerical algorithm for time-delayed singularly perturbed 2D convection-diffusion-reaction problem with two small parameters, Numer. Algor., 97(2) (2024), 687– 726
- [31] S. Priyadarshana, A. Padhan, and J. Mohapatra, Adaptive grid based moving mesh algorithms for singularly perturbed second-order Volterra integro-differential equations, Quaestiones Math., 48(7) (2025), 1007-1028.
- [32] S. Priyadarshana, J. Mohapatra, and S. R. Pattanaik, A second order fractional step hybrid numerical algorithm for time delayed singularly perturbed 2D convection-diffusion problems, Appl. Numer. Math., 189(6) (2023), 107–129.
- [33] S. Priyadarshana, J. Mohapatra, and L. Govindarao, An efficient uniformly convergent numerical scheme for singularly perturbed semilinear parabolic problems with large delay in time, J. Appl. Math. Comput., 68(1) (2022), 2617–2639.
- [34] S. Priyadarshana, J. Mohapatra, and H. Ramos, Robust numerical schemes for time delayed singularly perturbed parabolic problems with discontinuous convection and source terms, Calcolo, 61(1) (2024), 1-33.
- [35] M. Rahman, Integral Equations and Their Applications, WIT Press, 2007.
- [36] H. G. Roos, M. Stynes, and L. Tobiska, Numerical Methods for Singularly Perturbed Differential Equations, Springer, Berlin, 1996.
- [37] E. Sekar, Second order singularly perturbed delay differential equations with non-local boundary condition, J. Comput. Appl. Math., 417 (2023), 114498.



24 REFERENCES

[38] E. Sekar, L. Govindarao, J. Mohapatra, R. Vadivel, and N. T. Hu, Numerical analysis for second order differential equation of reaction-diffusion problems in viscoelasticity, Alexandria Eng. J., 92 (2024), 92–101.

- [39] S. Sevgin, Numerical solution of a singularly perturbed Volterra integro-differential equation, Adv. Differ. Equ., 2014 (2014), 171.
- [40] G. I. Shishkin and L. P. Shishkina, Difference Methods for Singular Perturbation Problems, Chapman and Hall, 2009.
- [41] M. Stynes and D. Stynes, Convection-Diffusion Problems, Graduate Studies in Mathematics, 2018.
- [42] M. Udupa, S. Saha, and A. Das, Computational analysis of blood flow through stenosed artery under the influence of body acceleration using Shishkin mesh, Int. J. Appl. Comput. Math., 8 (2022), 107.



